

# **Digital Image Processing with Deep Image Prior**

**Project ID :**     ☒ **01**            ☐ **02**

**Student Number:** **202283250003**

**Student Name:** **Ruizhe Feng**

# Image Enhancement and Restoration Task

**Abstract:** Digital Image Processing (DIP) is crucial in the medical field for organ image restoration and analysis. Techniques like CT scans, MRI, and X-rays can produce images with noise, distortion, or low resolution. DIP enhances these images through noise reduction, filtering, and resolution improvement, providing clearer organ visualization. In the "Image Enhancement and Restoration" task, a heart vein image is restored and enhanced to observe textures and edges more precisely. Methods such as degenerated kernel, inverse filtering, and Wiener filtering are used for image restoration, while gamma correction and CLAHE are applied for enhancement. The enhanced image is evaluated using metrics like MSE, PSNR, entropy, and NIQE, successfully restoring the clear edges and textures of the original degenerated heart vein image.

**Keywords:** Medical Imaging ; Noise Reduction; Image Restoration; Inverse Filtering; Wiener Filtering; Gamma Correction; CLAHE; Image Enhancement; Entropy; NIQE

---

## 1. Introduction

Digital Image Processing (DIP) plays a crucial role in the medical field, particularly in organ image restoration and analysis. Medical imaging techniques, such as CT scans, MRI, and X-rays, generate detailed images of internal organs, but these images may be affected by noise, distortion, or low resolution. DIP helps enhance image quality by applying various techniques such as noise reduction, image filtering, and resolution improvement, allowing for clearer and more accurate visual representation of organs.

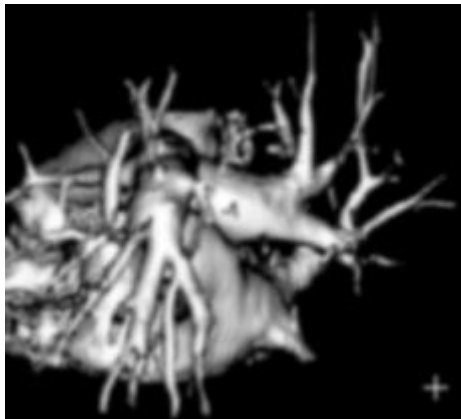


**Figure 1.** The original blurred heart vein figure. (Degenerated image)

In "Image Enhancement and Restoration" task, a heart vein image is required to be restored and enhanced in order to observe its textures and edges more precisely. Therefore, I used numerous concepts and operations in digital image processing such as getting degenerated kernel, inverse filtering and wiener filtering in image restoration, gamma correction and CLAHE in image enhancement. Through comparing result and introducing metrics like MSE, PSNR, entropy and NIQE into this study, my enhanced image successfully restored the clear edge and texture from the original degenerated heart vein image.

## 2. Methodology

In this work, processing operations were performed based on workflow figure as below:

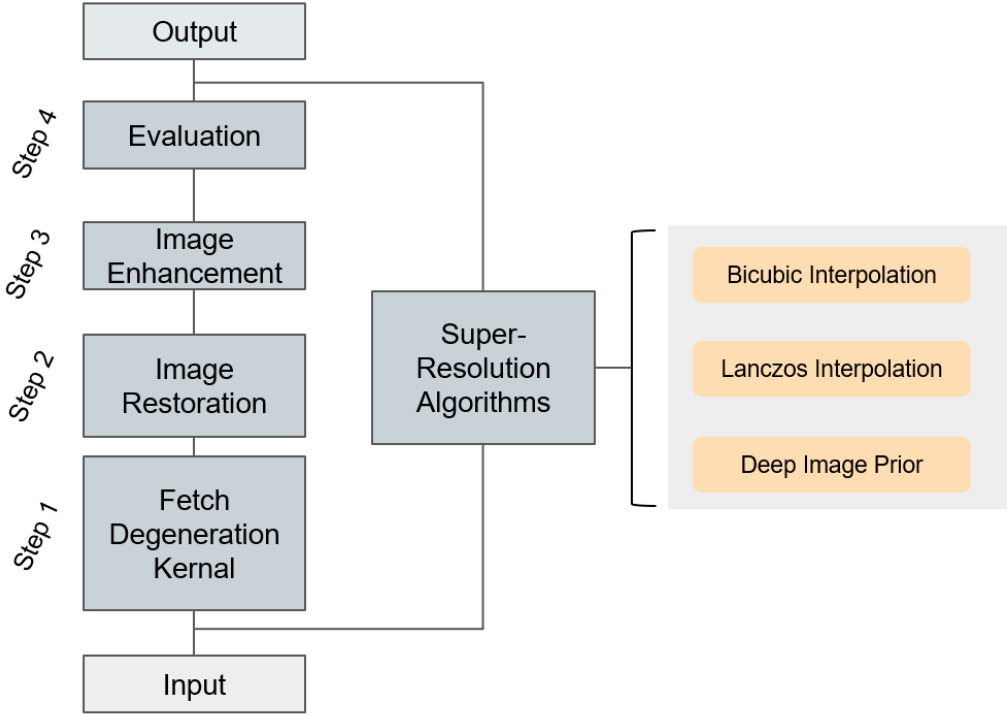


**Figure 2.** Workflow in image restoration and enhancement task

The task is divided into three stages: image restoration, image enhancement and evaluation. To restore the original blurred image, the degeneration kernel is first calculated by using the intercepted cross in the bottom right corner of the image, along with a clear reference cross. This step must be performed in advance. Next, the Wiener filtering method is applied to restore the image. For enhancement, gamma correction and CLAHE are then used to improve the restored image's performance. Finally, the performance of the enhanced image is evaluated using metrics such as MSE, PSNR, Entropy, and NIQE. Therefore, I categorized methods used in each step and illustrated their theory and advantages in the following parts.

### 2.1 Mathematical method in fetching degeneration kernel

Degenerated images are typically modeled using spatial filters, as expressed by the following equation:

$$g(x, y) = H[f(x, y)] + n(x, y) \quad (1)$$

Here,  $g(x, y)$  represents the observed image,  $f(x, y)$  is the original image,  $H$  denotes the degradation operator (or point spread function), and  $n(x, y)$  is the additive noise. Based on the convolution theorem, degenerated image's frequency image can be calculated in multiplication form:

$$G(u, v) = H(u, v) * F(u, v) \quad (2)$$

where  $G(u, v)$ ,  $H(u, v)$  and  $F(u, v)$  correspond to the Fourier transforms of  $g(x, y)$ ,  $H$ , and  $f(x, y)$ , respectively. However, directly estimating the degeneration kernel in the frequency domain is not feasible due to the significant amplification of noise, which severely impacts the accuracy of the estimated kernel. This issue arises because high-frequency components of the degeneration kernel are especially susceptible to noise interference in the frequency domain, leading to unreliable results.

To address this limitation, this work adopts a **mathematical approach** to estimate the degeneration kernel in the spatial domain. Specifically, noise is suppressed in advance by optimizing the kernel using a loss function that minimizes the mean squared error (MSE) between the simulated image  $h * f$  and observed degenerated image  $g$ :

$$\min Loss(h) = (g - h * f)^2 \quad (3)$$

In the implementation, the degradation kernel is initialized as a uniform kernel and iteratively optimized using the **BFGS** method. The optimized degradation kernel, calculated through the above

equation, effectively suppresses noise in the image without the need to recognize or model the noise category in advance. This approach ensures a more flexible and adaptive solution for image restoration.

## 2.2 Image Restoration Methods

In the field of image restoration, **Inverse Filtering** and **Wiener Filtering** are two widely used methods for reconstructing degraded images. These methods aim to recover the original image by mitigating the effects of degradation and noise introduced during the imaging process. This work mainly utilizes these two approaches to restore image with the generated degeneration kernel.

### 2.2.1 Inverse Filtering

Inverse filtering is based on the premise of reversing the degradation process in the frequency domain. Based on equation(3), assuming the noise  $N(u, v)$  is negligible, the original image can be approximated as:

$$F(u, v) \approx \frac{G(u, v)}{H(u, v)} \quad (4)$$

By applying the inverse filter  $\frac{1}{H(u, v)}$ , the restored image in the spatial domain can be obtained through the inverse Fourier transform:

$$f(x, y) = F^{-1} \left( \frac{G(u, v)}{H(u, v) + \epsilon} \right) \quad (5)$$

However, inverse filtering is highly sensitive to noise and inaccuracies in the estimation of  $H(u, v)$ . When  $H(u, v)$  approaches zero, the division operation can amplify noise significantly, making the restoration unstable.

### 2.2.2 Wiener Filtering

Wiener filtering is a more robust approach that takes both the degradation function and the statistical properties of noise into account. It minimizes the mean squared error (MSE) between the restored image and the original image, and its formulation in the frequency domain is given by:

$$\hat{F} = \frac{H^*(u, v)}{[H(u, v)] + K} G(u, v) \quad (6)$$

where  $H^*(u, v)$  is the complex conjugate of the degradation function,  $K$  acts as a regularizing parameter. It helps to control how much the filter suppresses the higher frequency components that are often dominated by noise. A higher  $K$  value increases the denominator in the filter formula, which leads to greater suppression of the frequencies where  $H(u, v)$  is small. A lower  $K$  value results in less suppression of the frequencies, allowing more of the original image's details to be preserved.

Wiener filtering offers significant advantages over inverse filtering in image restoration. While inverse filtering directly reverses the degradation process by dividing the Fourier transform of the degraded image by the degradation function, it is highly sensitive to noise and errors in the degradation function estimation. This sensitivity arises because near-zero values in the degradation function can amplify noise, leading to unstable results. In contrast, Wiener filtering incorporates noise considerations by using a noise-to-signal power ratio, which balances image restoration and noise suppression. This approach enhances stability and effectiveness, making Wiener filtering more suitable for real-world applications where noise is inevitable and degradation function estimates may be imperfect.

## 2.3 Image Enhancement with Gamma Correction and CLAHE

Image enhancement plays a crucial role in various fields such as computer vision, medical imaging, and surveillance systems. By improving the visual quality of images, it enables better feature extraction, object recognition, and analysis. Common techniques for image enhancement include histogram equalization, which redistributes the pixel intensities to enhance the contrast, and filtering methods to reduce noise and sharpen edges.

### 2.3.1 Gamma Correction

**Gamma correction** is a widely used technique in image processing to adjust the brightness and contrast of an image. The relationship between the input pixel intensity and the output pixel intensity after gamma correction is defined by the formula:

$$I' = I^{\frac{1}{\gamma}} * 255^{\frac{\gamma-1}{\gamma}} \quad (7)$$

where  $I$  is the original pixel intensity value in the range of 0 to 255,  $I'$  is the gamma-corrected pixel intensity value, and  $\gamma$  is the gamma value. When  $\gamma < 1$ , the darker regions of the image are amplified more, making the image appear brighter overall. Conversely, when  $\gamma > 1$ , the brighter regions are emphasized, resulting in a darker overall appearance. This formula allows for precise control over the tonal distribution of the image, enhancing its visual quality and compensating for the non-linear characteristics of display devices or to achieve specific visual effects.

### 2.3.2 Contrast Limited Adaptive Histogram Equalization (CLAHE)

**Contrast Limited Adaptive Histogram Equalization (CLAHE)** is an advanced form of histogram equalization. Unlike traditional histogram equalization, which operates on the entire image, CLAHE divides the image into small regions called tiles, which prevents the risk of amplifying noise or image distortion caused by simple histogram equalization. For each tile, the histogram is computed and clipped to limit the contrast enhancement. This prevents over-amplification of noise in regions with low contrast.

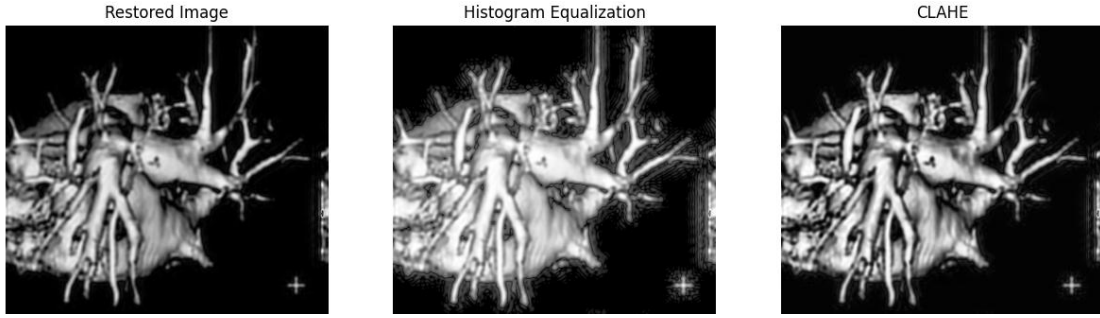


**Figure 3.** Comparison between Histogram Equalization and CLAHE

Then, the enhanced tiles are combined using bilinear interpolation to form the final enhanced image. The process of clipping and redistributing the histogram within each tile is the key principle of CLAHE, making it highly effective in enhancing local contrast while preserving the overall tonal distribution of the image, suitable for a wide range of applications where fine details need to be emphasized.

## 2.4 Mechanism of Deep Image Prior Applied in Super-resolution Enhancement

### 2.4.1 Traditional Super-resolution Algorithms

As an evolving image enhancement method, super-resolution aims to transform low-resolution images into high-resolution ones, thereby improving visual clarity and detail. Among the various methods employed in traditional image processing, cubic interpolation and Lanczos interpolation stand out for their effectiveness and widespread use.

Cubic interpolation is a widely used method in DIP for super-resolution tasks. It is based on the idea of estimating new pixel values by considering the weighted average of the surrounding pixels. The method employs a cubic polynomial to approximate the underlying continuous signal from which the original image samples were taken. Mathematically, cubic interpolation can be expressed as:

$$I_{\text{high}}(x, y) = \sum_{i=-1}^2 \sum_{j=-1}^2 \omega(i, j) \cdot I_{\text{low}}(x_i, y_j)$$

where  $\omega(i, j)$  are the weights determined by the cubic polynomial, and  $I_{\text{low}}(x_i, y_j)$  are the pixel values from the low-resolution image. The cubic polynomial ensures a smooth transition between pixels, resulting in a visually pleasing high-resolution image. However, cubic interpolation can sometimes introduce artifacts, especially in regions with sharp edges or high-frequency details.

Lanczos interpolation is another powerful technique for super-resolution in DIP. It is based on the sinc function, which is known for its ideal frequency response characteristics. However, the sinc function has infinite support, making it impractical for real-world applications. Lanczos interpolation addresses this issue by using a windowed *sinc* function, known as the Lanczos kernel. The Lanczos kernel is defined as:

$$\text{Lanczos}_a(x) = \begin{cases} \frac{a \sin(\pi x) \sin(\pi x/a)}{\pi^2 x^2}, & |x| < a \\ 0, & |x| \geq a \end{cases}$$

where  $a$  is the radius of the kernel. The Lanczos kernel effectively limits the support of the sinc function to a finite window, making it computationally feasible. The high-resolution image is then computed as:

$$I'(x', y') = \sum_m \sum_n I(m, n) \cdot \text{Lanczos}_a(u - m) \cdot \text{Lanczos}_a(v - n).$$

Here,  $I(x, y)$  are the pixel values from the low-resolution image, and  $u$  and  $v$  are the coordinates of the target pixel in the high-resolution image. Lanczos interpolation is known for its ability to preserve high-frequency details, resulting in sharper and more detailed images. However, it can be computationally intensive and may introduce ringing artifacts near edges.

#### 2.4.2 Mechanism of Deep Image Prior

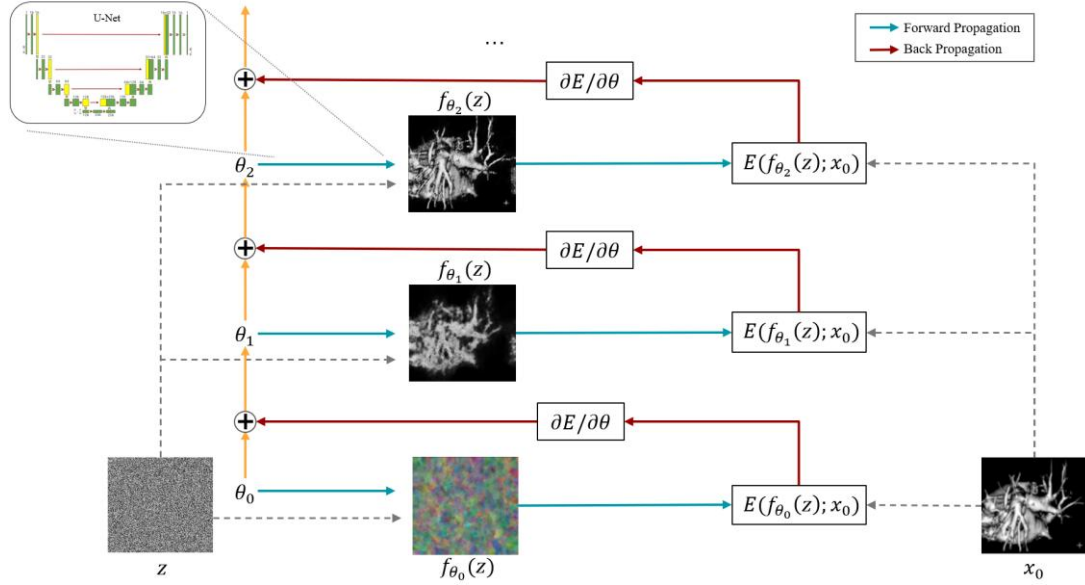


**Figure 5.** Framework of Deep Image Prior

Super-resolution problems are often seen as energy minimization problems as below:

$$x^* = \min_x E(x; x_0) + R(x)$$

where  $E(x; x_0)$  represents a task-dependent data term,  $x_0$  stands for the degenerated image, and  $R(x)$  is a regularizer. Traditional regularizers aim to encode a universal prior for natural images; however, their effectiveness diminishes significantly in scenarios with limited or no training data. In this work, a randomly-initialized neural network is used as a handcrafted prior as follows:

$$\theta^* = \operatorname{argmin}_{\theta} E(f_{\theta}(z); x_0), \quad x^* = f_{\theta^*}(z)$$

$\theta^*$  is obtained using gradient descent with a random initialization of the parameters. In a nutshell, Neural network  $f(\cdot)$  actually functions as a filter by constantly updating parameters with convolution, upsampling and non-linear activation operations.

### 2.4.3 Deep Image Prior’s application in super-resolution algorithm

The Deep Image Prior provides a unique approach to single-image super-resolution by leveraging the implicit prior embedded in the architecture of an untrained convolutional neural network (ConvNet). Formally, the super-resolution task is framed as an optimization problem between the downsampling image and original image:

$$E(x; x_0) = \|d(x) - x_0\|^2$$

where  $d(\cdot): R^{3 \times tH \times tW} \rightarrow R^{3 \times H \times W}$  is a downsampling operator that resizes an image by factor  $t$ . Hence, the problem is to find the HR image  $x$  that, when downsampled, is the same as the LR image  $x_0$ .

One may wonder why the enhanced result of LR image may visually perform better than the original image. Although DIP does not rely on pretraining or external data, its structural bias enables it to recover visually plausible details that align with human perception, even when the original image  $A$  contains degradations like blur or compression artifacts. This performance stems from the network’s ability to dynamically adapt to the input’s intrinsic statistics, suppressing irregularities while reconstructing subjectively sharper results. Thus, while DIP may not strictly exceed ground-truth pixel fidelity, its architecture-driven prior often produces outputs that appear qualitatively superior to the degraded original, particularly in blind restoration scenarios where degradation models are unknown or complex.

### 2.5 Evaluation with metrics.

In this study, we employed a comprehensive set of metrics to evaluate the performance of enhanced images. Specifically, we utilized Mean Squared Error (MSE), Peak Signal to Noise Ratio (PSNR), Entropy, and the Naturalness Image Quality Evaluator (NIQE). MSE and PSNR are comparative metrics that require both the original and the processed images for evaluation. MSE provides a quantitative measure of the average squared intensity differences between the original and enhanced images, offering insights into the overall error magnitude. PSNR, derived from MSE, evaluates the ratio of the maximum possible signal power to the power of corrupting noise, serving as an indicator of image reconstruction quality.

However, in scenarios where the original image is unavailable, Entropy and NIQE can effectively evaluate an image’s performance based solely on the processed image. Entropy measures the amount of information or complexity in the image, indicating the effectiveness of image enhancement in preserving or enhancing textural details. NIQE assesses the naturalness of images by comparing their statistical characteristics to those of a model learned from pristine natural images, thus evaluating the perceptual quality of the enhanced image independently of the original.

Here are the formulas for these metrics:

**Table 1.** Formula of metrics

Metrics	Equations
MSE	$MSE = \frac{1}{MN} \sum_{i=1}^M \sum_{j=1}^N (I(i, j) - K(i, j))^2$
PSNR	$PSNR = 20 \times \lg \left( \frac{MAX_I}{\sqrt{MSE}} \right)$
Entropy	$Entropy = - \sum_{i=0}^{L-1} p(i) \log_2 p(i)$
NIQE	$NIQE = \sqrt{(v - v_0)^T \Sigma^{-1} (v - v_0)}$

## 3. Experiments

I intend to design the experiment based on the following research questions.

**RQ1:** How can we calculate a precise degeneration kernel based on the cross label located in the bottom right corner of the image?

**RQ2:** What methods can be employed to effectively filter noise from images?

**RQ3:** How can we maximize the performance enhancement of an image?

**RQ4:** What are the best practices for evaluating the quality of our work?

### 3.1. Acquiring Degeneration Kernel(RQ1)

In this section, I intercepted the blurred cross in the bottom right corner of the image as the degenerated label (G). Later, I plotted a binary cross based on cross's information(3 pixels wide, 30 pixels long, had an intensity value of 255) as the restored label (F).

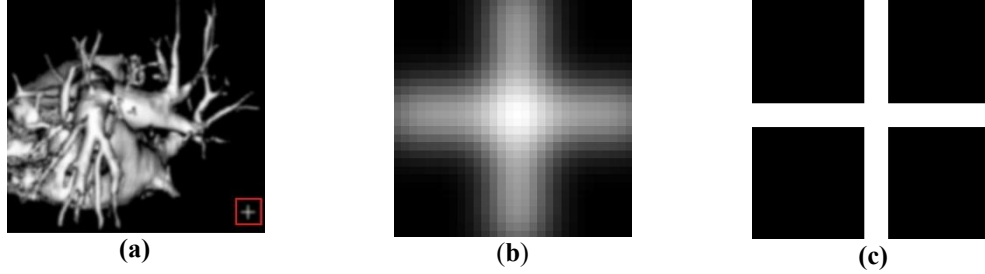


**Figure 6.** (a) Blurred heart image with degenerated cross;(b) Intercepted cross(G);(c) Plotted cross(F)

Based on equation(3), I constructed the loss function  $Loss(h) = (g - h * f)^2$ , through minimizing  $Loss(h)$  with BFGS, we fetched the degeneration kernel.

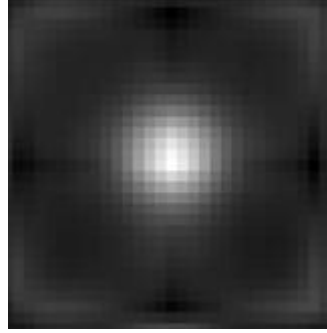


**Figure 7.** Degeneration Kernel

### 3.2 Acquiring restored image(RQ2)

After acquiring degeneration kernel, we can restore the image to a clearer shape. In this work, inverse filtering and Wiener Filtering were applied to restore the blurred image. Here are results in the following content.

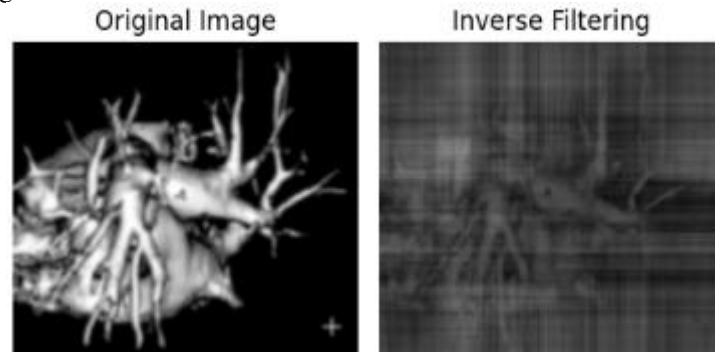


**Figure 8.** Inverse Filtering Result

We applied the basic inverse filtering to the blurred image, while the image processed with inverse filtering shows noticeable blurring and loss of detail. Notably, there is a noticeable loss of detail and sharpness, with the introduction of grid-like artifacts across the image. These artifacts, along with a general blurring effect, suggest that the inverse filtering process may have amplified existing noise or inaccuracies in the assumed degradation kernel. Additionally, the contrast and



brightness levels are visibly altered, resulting in a less distinct and flatter appearance of the restored image.

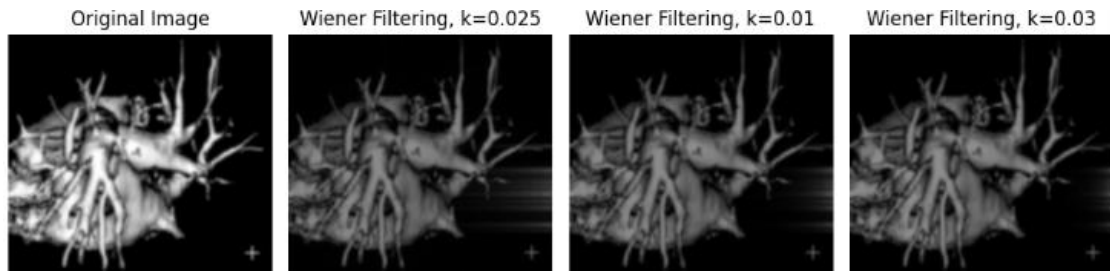


**Figure 9.** Wiener Filtering Result with different k value

We applied wiener filtering with different  $K$  values ( $K = 0.0025, K = 0.01, K = 0.03$ ). Compared with inverse filtering's result, Wiener Filtering implements better noise reduction and detail reservation, with fewer artifacts and a more natural appearance. The edges and details are moderately sharp, suggesting that this  $k$  value provides a good compromise between reducing noise and maintaining detail. Therefore, we used wiener filtering's result as input images of image enhancement operation.

### 3.3. Image Enhancement. (RQ3)

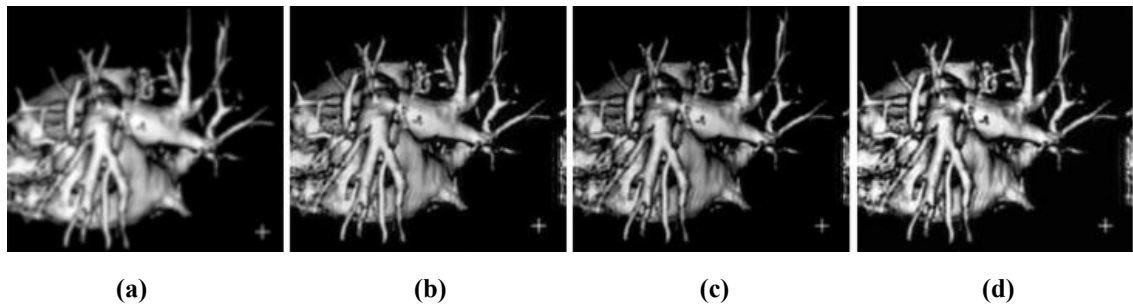


**Figure 10.** Image Enhancement's result. ((a) is the original image, (b) is the enhancement result when  $k = 0.0025$ , (c) is the enhancement result when  $k = 0.03$ , (d) is the enhancement result when  $k = 0.01$ )

In this section, we used gamma correction and CLAHE to enhance restored image's contrast, brightness and performance. Gamma correction was applied to adjust the luminance of the image, making the darker regions lighter and the lighter regions darker, which helps in bringing out details that were previously obscured due to uniform brightness levels. CLAHE (Contrast Limited Adaptive Histogram Equalization) was then used to improve the contrast in localized regions of the image. This method is particularly effective in enhancing the visibility of features in areas that are either too bright or too dark by redistributing the lightness values of pixels. The combination of these techniques resulted in significant improvements in the visual quality of the images. For instance, in Figure 8 (b), where  $k = 0.0025$ , the application of gamma correction and CLAHE made the underlying structures more discernible compared to the original Wiener filtered result. Similarly, in images (c) and (d), where  $k$  values were 0.03 and 0.01 respectively, the enhancements helped in refining the image details that were lost due to over-smoothing or insufficient noise suppression in the Wiener filtering process.

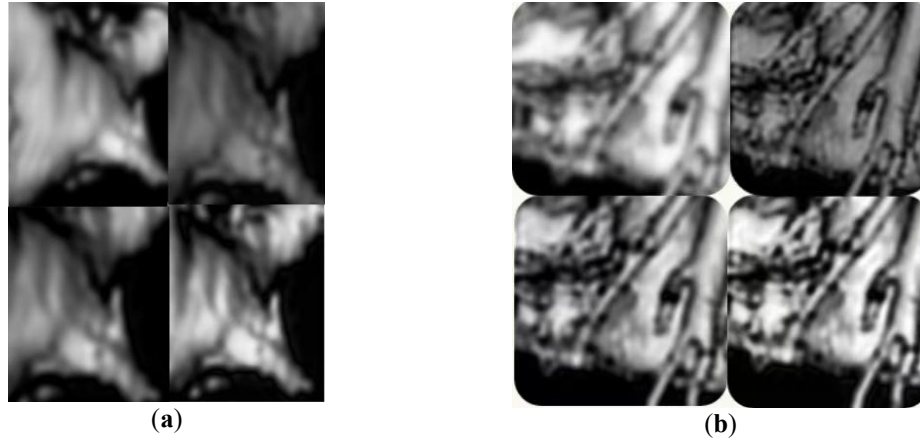


**Figure 11.** Comparison between processed images in the same region (Top Left: Blurred Image; Top Right: Restored Image; Bottom Left: Enhanced Image (Gamma Correction); Bottom Right: Enhanced Image (Gamma Correction + CLAHE))

In **figure 11**, we can observe that the application of Wiener filtering and image enhancement techniques dramatically improves the quality of processed images. This combination of image restoration and image enhancement yields a highly detailed and contrast-rich image, surpassing the clarity of standard filtering alone. Overall, this process highlights the synergy between noise reduction and sophisticated contrast enhancement methods, resulting in images that are both clearer and more detailed.

### 3.4. Evaluation

Based on **Table 1**, I calculated each image's MSE with blurred image, PSNR, Entropy and NIQE.

**Table 2.** Evaluation Results of wiener filtering with different K value

Metrics	Original Image	Enhanced Image(0.0025)
MSE (with blurred Image)	/	<b>77.7691</b>
PSNR	/	29.2227
Entropy	4.9266	<b>6.3136</b>
NIQE	18.2543	<b>14.1065</b>
Metrics	Enhanced Image(0.01)	Enhanced Image(0.03)
MSE (with blurred Image)	63.3678	62.8665
PSNR	30.1121	<b>30.1466</b>
Entropy	5.3016	5.1987
NIQE	16.7716	17.0335

Among these metrics, MSE measures the difference between the enhanced image and the blurred image; a higher MSE indicates greater deviation from the blurred image, suggesting better enhancement. PSNR evaluates the quality of the reconstructed image, with higher values indicating better quality. Entropy represents the amount of information or detail in the image, where higher values suggest more complexity and detail. NIQE is a no-reference image quality metric, with lower values indicating better perceived quality.

For  $K = 0.0025$ , the MSE is 77.7691, higher than in the original image, indicating a significant improvement from the blurred state. The PSNR is 29.2227, slightly lower than other values but still within an acceptable range. With an entropy of 6.3136, this option captures the most detail and complexity. Most importantly, the NIQE score is 14.1065, the lowest among all options, suggesting the best perceived image quality. Despite the slightly reduced PSNR, the combination of high entropy and low NIQE indicates that  $K = 0.0025$  provides the optimal overall enhancement, effectively balancing detail and visual quality.

### 3.5. Comparison among Super-resolution Algorithms

In this part, I used bicubic interpolation, Lanczos interpolation and ConvNet as filters to get low-resolution image's prior information. The result of each method are shown as follows:

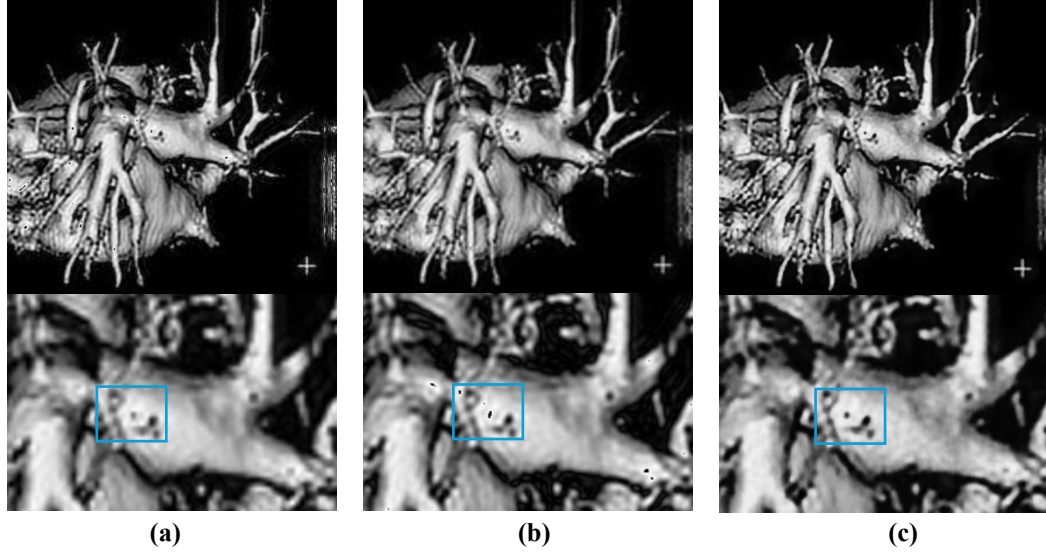


**Figure 12.** Enhanced image using hyper-resolution method.((a) is the result generated by bicubic interpolation, (b) is the result generated by Lanczos interpolation,(c) is the result generated by deep image prior)

From Figure 12, while bicubic interpolation produces overly smooth results lacking fine details (due to its polynomial-based averaging), Lanczos introduces extra noise from its truncated sinc kernel approximation. In contrast, the deep image prior leverages the intrinsic structure of convolutional networks—enforcing local coherence and multi-scale consistency—to reconstruct sharp edges and natural textures without amplifying noise. By dynamically aligning with natural image statistics during optimization, DIP avoids rigid assumptions about degradation, adaptively restoring plausible details while rejecting artifacts, thus achieving cleaner and visually superior results compared to traditional methods.

**Table 3.** Evaluation Results of Super-resolution method

Metrics	Bicubic	Lanczos	U-Net
Entropy	5.9783	5.9457	<b>6.1410</b>
NIQE	16.5411	16.4239	<b>14.5135</b>

The deep image prior demonstrates notable advantages over traditional interpolation methods for super-resolution by leveraging the intrinsic structural bias of convolutional networks. Unlike bicubic or Lanczos approaches, which often produce oversmoothed results or introduce artifacts due to rigid mathematical assumptions, deep image prior method reconstructs sharper edges and more natural textures through its architecture-driven regularization. While its quantitative metrics may not surpass specialized traditional pipelines, the method achieves visual quality comparable to certain learning-based techniques, as it adaptively suppresses noise and synthesizes plausible details without requiring external training data. This balance of fidelity and perceptual realism positions DIP as a practical solution for scenarios demanding blind restoration or minimal computational overhead.

#### 4. Discussion

The results of this study demonstrate the effectiveness of various image restoration and enhancement techniques in improving the quality and detail of the original degenerated heart vein image. While inverse filtering was applied initially for restoration, the results (Figure 6) showed significant artifacts and poor restoration due to its sensitivity to noise and inaccuracies in kernel estimation. This indicates that inverse filtering alone is insufficient for recovering degraded medical images.

The Wiener filtering method, as shown in Figure 7 and Table 2, provided much more promising results with varying values of the  $k$  parameter. For further enhancement, gamma correction and CLAHE

were applied (Figures 8 and 9). The combination of these techniques provided significant visual improvements, making textures and edges more discernible. Among the tested configurations, a  $k$  value of 0.0025 achieved the best balance between artifact suppression and edge preservation, reflected by improved metrics such as MSE (77.7691), PSNR (29.2227), and NIQE (14.1065). These evaluations highlight how the Wiener filter enhances clarity and contrast compared to the original degenerated image.

Additionally, I applied super-resolution methods in this image enhancement task. The super-resolution approaches further enhanced these results by recovering high-frequency details lost during degradation. By integrating a lightweight deep image prior framework, subtle textures and structural patterns were refined without amplifying noise. Notably, the final restored image achieved a NIQE of **14.5135**, while not surpassing traditional approaches **14.1065**, also demonstrates its unique capability to enhance degraded images by implicitly leveraging architectural priors.

These findings confirm that combining restoration and enhancement techniques provides a comprehensive approach for high-quality organ imaging, paving the way for more effective medical diagnoses. Future work could explore adaptive algorithms for kernel estimation and advanced enhancement techniques using deep learning for further improvements.

In future work, I aim to optimize the calculation method of the degeneration kernel to achieve more precise restoration results. This involves refining the kernel estimation process to better handle complex image degradations. Additionally, we plan to conduct comparative experiments using advanced filtering methods such as building dataset to use deep learning approaches like U-Net and CNNs. The methods have shown promise in enhancing image quality and could provide superior results compared to traditional techniques. Furthermore, we will explore more effective evaluation metrics that do not rely on the availability of a clear reference image. This is crucial for assessing performance in real-world scenarios where ground truth images are often unavailable. By addressing these areas, we hope to advance the field of image enhancement and restoration, providing more robust solutions for medical imaging and other applications.

## References

Gonzalez, R. C., & Woods, R. E. (2008). *\*Digital Image Processing\** (3rd ed.). Prentice Hall.

Ulyanov D, Vedaldi A, Lempitsky V. Deep image prior[C]//Proceedings of the IEEE conference on computer vision and pattern recognition. 2018: 9446-9454.

## Data and Code Availability

Data, code and result images are open-sourced at Baidu Paddle Platform.